3D NUMERICAL STUDY OF MHD FLOW IN A RECTANGULAR DUCT WITH A FLOW CHANNEL INSERT

Damien Sutevski, Sergey Smolentsev, Neil Morley, Mohamed Abdou

UCLA Fusion and Technology Center: 420 Westwood Plaza, Los Angeles, CA 90095-159, Damien@fusion.ucla.edu

This study continues our ongoing investigation of magnetohydrodynamic (MHD) flows in poloidal ducts of the Dual-Coolant Lead-Lithium (DCLL) blanket with an insulating flow channel insert (FCI). We report our first 3D modeling results for an approximately ideally non-conducting FCI. The FCI and duct geometry match those of an experiment performed recently in Southwestern Institute of Physics (SWIP), China. The experimental FCI is made of epoxy and has a pressure equalization slot (PES) in one wall, which is perpendicular to the applied magnetic field. Previous 2D modeling efforts based on the fully developed flow model have demonstrated a significant difference with the experimental results in the MHD pressure drop, indicating 3D effects may be significant. The new 3D results, obtained with an unstructured, parallel MHD solver HIMAG, are in fair agreement with the experimental data. These results confirm a substantial reduction in MHD pressure drop by the FCI, but not as significant as would be expected under fully developed flow conditions.

I. INTRODUCTION

Pressure drops in magnetohydrodynamic (MHD) flows can be very significant. Fusion reactor blanket designs are subject to this effect, so solutions are sought for alleviating the losses. The US dual-coolant lead-lithium (DCLL) blanket design, shown in Fig. 1, therefore features a silicon carbide (SiC) flow channel insert (FCI), and its purpose is to electrically insulate the bulk flow reducing the MHD pressure drop as well as to thermally insulate the flow from losses to the surrounding helium flows.[1,2,3] Previous results from a 2D numerical study as well as experiments conducted at the Southwestern Institute of Physics in China have validated this benefit.[4,5] For pressure equalization between the bulk and gap flows, pressure equalization holes (PEH) or slots (PES) have been suggested. In this study, we focus on an FCI with a PES.

This study reproduces the previous works' configurations[4,5] but instead utilizes a recently developed 3D numerical code to solve the flow behaviors.

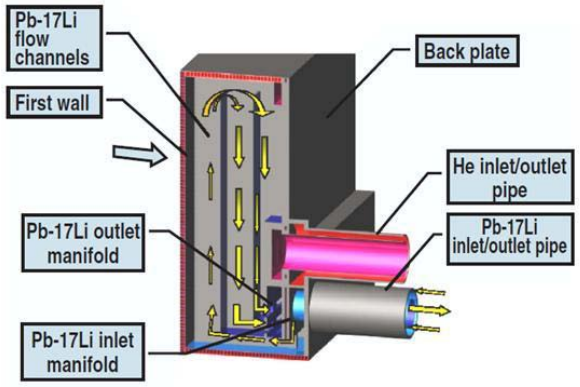

Fig. 1. Sketch of the US DCLL DEMO blanket with insulating FCI.

I.A. Experiment in China and 2D numerical study

An experiment in China at the Southeastern Institute of Physics has been conducted.[5] All dimensions and material properties in the experiment have been matched in this study. Additionally, 2D numerical analysis, incorporating a fully-developed flow model, has been carried out at UCLA.[4]

Both studies have confirmed a reduction in pressure drop due to the FCI. However, there were significant discrepancies in the pressure drops between the two cases. These differences will be visually portrayed later in the paper.

Here we model and solve the same problem using HIMAG, a 3D, unstructured, parallel MHD solver with the goal of resolving the pressure discrepancy and investigating the phenomena responsible.

I.B. HIMAG, a 3D MHD numerical code

HIMAG, an abbreviation for **H**yPerComp **I**ncompressible **M**HD solver for **A**rbitrary **G**rids, is an MHD solver that has been developed over several years by Hypercomp in conjunction with UCLA. The primary objective of HIMAG is to solve 3D MHD incompressible and free surface flow problems and is well suited for solving closed channel flows within the DCLL. It

features a parallel iterative solver, arbitrary mesh structures, implicit algorithms, and a choice of **φ** and **B** formulations. However, HIMAG does not account for instabilities that may lead to turbulence which is a feature that should be considered in the future.

II. PROBLEM SPECIFICATIONS

Conditions within a DCLL, such as in ITER, DEMO, or a power reactor, are extraordinarily complex and include the following features: 3D magnetic field components, fringing magnetic fields, buoyancy and gravity effects, turns, obstacles (such as the FCI), converging and expanding sections, and MHD turbulence.

In this numerical experiment, we have simplified the reactor conditions to consider a rectangular duct with laminar flow and a transverse fringing magnetic field and a nearly ideally insulating FCI.

The related configuration information is summarized in Fig. 2. The fluid is an Indium-Galium-Tin (In-Ga-Sn) eutectic with a density, ρ_l = 6,350 kg/m^3, a viscosity, ν = 3e-7 m^2/s, and an electrical conductivity, σ_l = 3.34e6 S/m. The outer duct is 1500 mm long and is made of stainless steel with an electrical conductivity, σ_D = 1.4e6 S/m. Contained within is a 1000 mm FCI, constructed of epoxy with a modeled electrical conductivity, σ_{FCI} = 0.1 S/m. An applied magnetic field varies from B = 0 to B_0 T, where the maximum strength B_0 is varied, and its fringing field lies entirely within the FCI's range. It is further described in Section II.A. The Reynolds number (Re) is 5000, and the Hartmann number (Ha) varies from approximately 1200 to 2500. Respectively, they are defined by:

$$Re = \frac{UL}{\nu}, \qquad (1)$$

$$Ha = BL\sqrt{\frac{\sigma}{\rho\nu}}. \qquad (2)$$

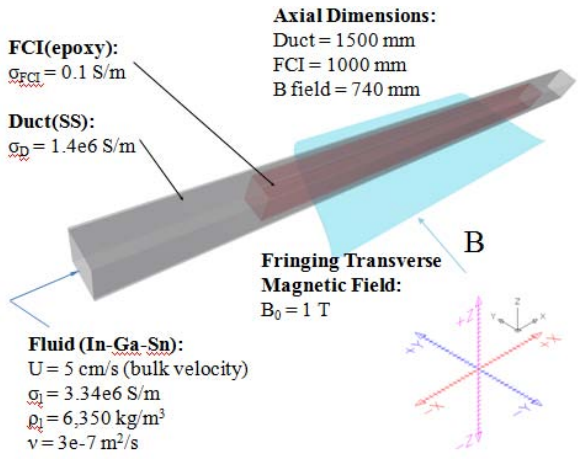

Fig. 2. Material properties and configuration of the setup.

II.A. Boundary, Mesh, and Computational Conditions

The following boundary conditions are applied: **n** • **j** = 0 at all outer surfaces, U = 5 cm/s at the inlet, and ∂**u**/∂x = 0 and P = 0 at the outlet where **n** is the vector normal, **j** is the current density, and P is the pressure. A no-slip condition is also applied to fluid-solid interfaces while a symmetry boundary is applied at the x-z mid-plane.

A 5.2 million element grid was constructed using HIMAG's grid generator with 508, 92, and 56 cells in the x, y, and z directions. The grid is shown in Fig. 3 where Ha and sidewall layers and fringing magnetic field zones have increased resolution. The grid was partitioned, and the simulation was run in parallel over 64 cores.

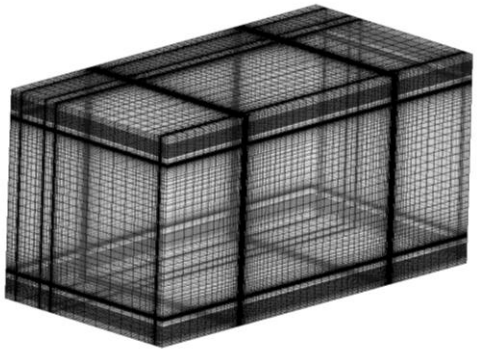

Fig. 3. Example of the computational mesh used in the simulation shown with a distorted aspect ratio.

The magnetic field strength, to change the Ha number, and FCI electrical conductivity were changed over the runs. Though electrical conductivities greater than σ = 0.1 S/m are more likely in practice, we have intentionally left these results for later considerations. In addition to the reference configuration, some runs were performed with an FCI without a slot.

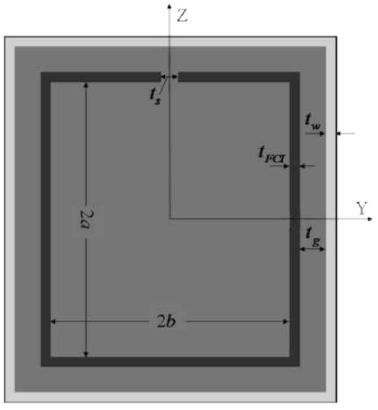

Fig. 4. The cross section of the duct with the FCI and pressure equalization slot.

TABLE I. Cross-section Dimensions

Dimensions	Notation	Length [mm]
Half-width of FCI box	b	23
Half-height of FCI box	a	27
FCI thickness	t_{FCI}	2
Thickness of gap	t_g	5
Thickness of slot	t_s	3
Thickness of the Fe wall	t_w	2

II.B. Cross-sectional Dimensions

The characteristic length used as a linear scale to change to dimensionless parameters is $L = b + t_{FCI} + t_g$.

II.C. Magnetic Field Description

The magnetic field strength is defined by Eq. (3) below:

$$B = \begin{cases} 0, & |x| > 435\ mm \\ \frac{B_0}{2}\left[sin\left(\frac{\pi(x \pm 435)}{w} - \frac{\pi}{2}\right) + 1\right], & 435 > \mp x > 305\ mm \\ B_0, & |x| < 305\ mm \end{cases} \quad (3)$$

where B_0 is the maximum strength, which ranges from 1 to 2 T in the simulations, and the width of the fringing field, w = 130 mm. The field is shown in Fig. 5. It is prescribed numerically by an electric potential formulation.

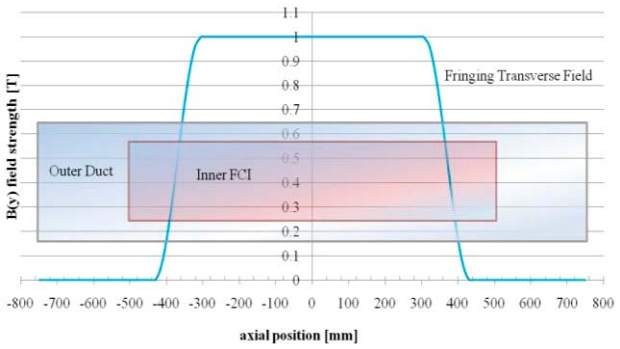

Fig. 5. The magnetic field strength is shown here with an outer duct and FCI overlay for perspective.

III. RESULTS

First, we inspect the velocity profile in the ducts with an FCI having a slot and having no slot. The profiles are measured at the x = 0 plane, in the middle of the duct, where the flow is the closest to the fully developed one. In Fig. 6, an M-shape profile, typical to MHD flows, can be seen. Although the bulk flow within an insulating duct is generally not expected to show this behavior, it is common for duct flows with a fringing magnetic field.[6] The large negative velocity is that within the FCI slot. It reduces the strength of the "upper" M-shape.

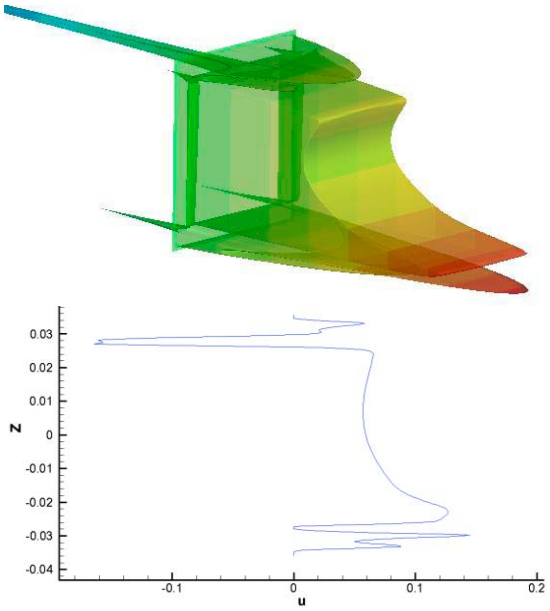

Fig. 6. The velocity profiles where the FCI has a slot in units of m/s, and the Z-axis in m.

Similarly, in Fig. 7, there is an M-shape profile, again characteristic of flow in a fringing magnetic field. However, without an FCI slot, the flow is symmetric.

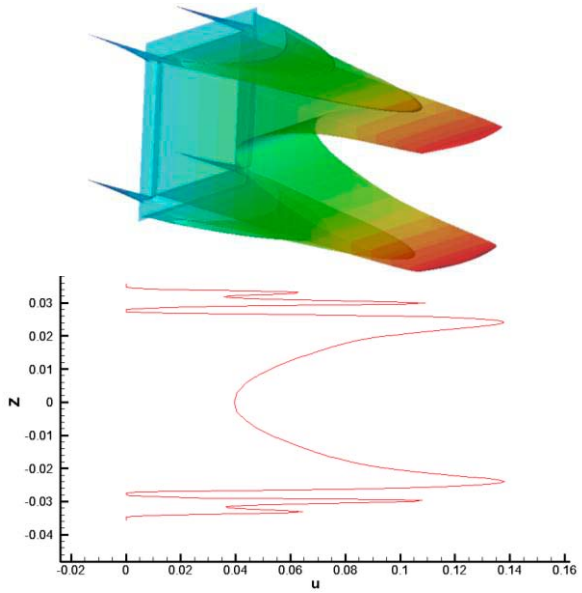

Fig. 7. The velocity profile where the FCI has no slot in units of m/s, and the Z-axis is in m.

Both Fig. 6 and 7 contain asymmetric M-shape velocity profiles within the upper and lower gaps. This asymmetry is due to the difference between the electrical conductivities of the wall and FCI. Flow in gaps that are perpendicular to the magnetic fields appear to be stagnant are not shown here.

Pressure drops in the simulations were calculated similarly to those in the Chinese experiment. These measurements in the experiment were taken in the gap between the duct and FCI at the opposite side of the slot. Here we represent the normalized pressure drops with a pressure drop coefficient ξ which is calculated by (Ref. 4):

$$\xi = -\frac{\frac{dp}{dx}L}{\rho_l U^2} \qquad (4).$$

Fig. 8 compares the pressure coefficients between the experimental, 2D, and 3D computations. There are also two data points from the no-slot case of the 3D run for comparison. The 3D computations agree well with experimental results and suggest that the discrepancy between the 2D and experimental numbers are due to 3D effects.

It could be possible that the primary 3D effect in the discrepancy is the leakage of axial currents from the bulk flow into the slot. Inspecting a volumetric rendering of the axial current distribution corroborates that, as shown in Fig. 10. This figure illustrates only the strongest axial currents and is for presented for qualitative inspection. Strong axial currents expectedly lie within the fringing field zones, but significantly strong axial currents are shown leaking axially along the length of the slot. Due to complexity of the 3D currents, we have no current line plot that sufficiently supports this.

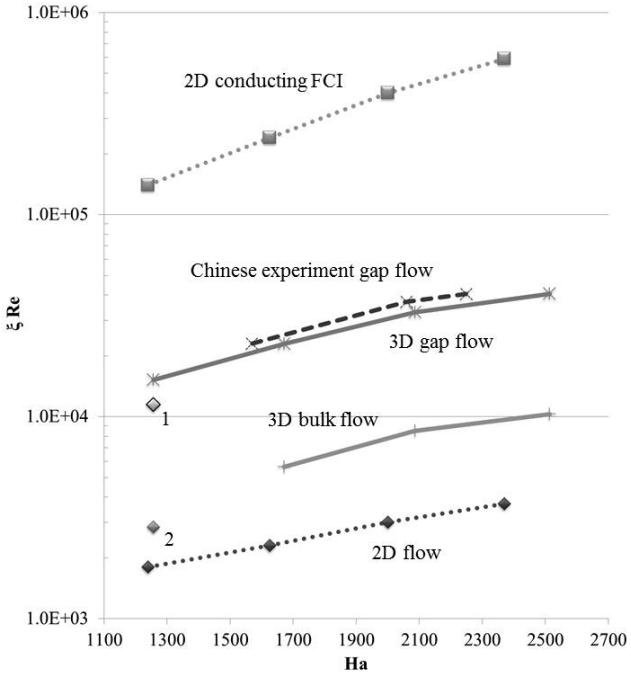

Fig. 8. Comparisons of the pressure drop coefficients versus Ha number for the experimental, 2D, and 3D cases with two numbered data points:
1: 3D gap flow without slot,
2: 3D bulk flow without slot.

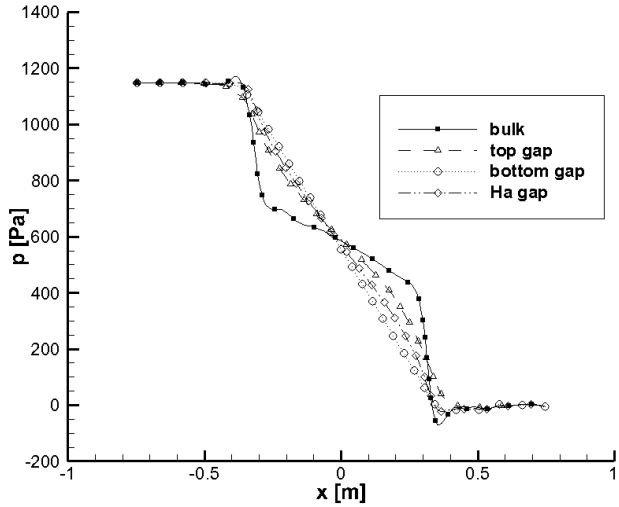

Fig. 9. Various comparisons of the pressure drop versus position for the 3D case with a slot.

However, referring to Fig. 8, the elimination of the FCI slot does not appear to drastically change the pressure drop from that of the slotted case. Since slot leakage is no longer possible, this effect may suggest that the length of the channel between the fringing fields is not adequate for the flow to fully develop. Fig. 9 may also support this conclusion. We can see that the linear pressure drop within the gaps is not matched by the bulk flow. It may indicate that the slot width is not adequate in hydrodynamically coupling the duct and slot flows.

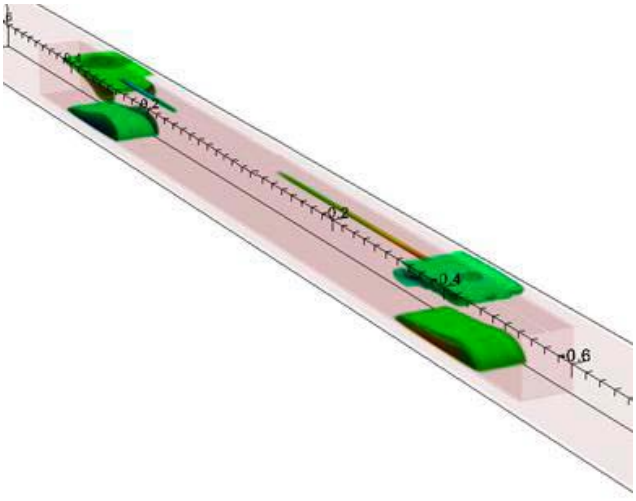

Fig. 10. Volume rendering of the axial current distribution.

IV. CONCLUSIONS

The pressure drop coefficients computed for the 3D case match well with the experimental results. The results suggest that the earlier observed discrepancy between the 2D and the experimental pressure drop coefficient is due to 3D effects. These are indicated by: the axial currents, which can be found not only in the fringing field regions but also in the middle section of the duct; M-shaped velocity profiles, which can be observed even in the case without the pressure equalization slot; and significant difference in the MHD pressure drop between the bulk flow and that in the gap (if the flow is fully developed, the pressure should be uniform over the whole cross-sectional area). In both the computations with and without the slot, currents also showed a tendency to move axially in the FCI interior corners (not pictured). In the no slot case, the pressure drop coefficient in the bulk flow approaches that for the 2D fully developed flow as expected. In this case, the bulk flow is decoupled from the gap flow but still exhibits an extra pressure drop from 3D effects. Further study to fully comprehend the nature of the current circuits is necessary.

REFERENCES

1. S. SMOLENTSEV, N. MORLEY, M. ABDOU, *MHD and Thermal Issues of the SiCf/SiC Flow Channel Insert*, Fusion Science and Technology, 50, 107-119 (2006).
2. S. MALANG, E. BOJARSKY, L. BÜHLER, H. DECKERS, U. FISCHER, P. NORAJITRA, H. REISER. Dual coolant liquid metal breeder blanket. In Proceedings of the 17th Symposium on Fusion Technology (Rome, Italy, September 14-18, 1992), pp. 1424-1428.
3. C.P.C. WONG, S. MALANG, M. SAWAN, M. DAGHER, S. SMOLENTSEV et al., An overview of dual coolant Pb-17Li breeder first wall and blanket concept development for the US ITER-TBM design. *Fusion Eng. Des*., vol. 81 (2006), pp. 461-467.
4. S. SMOLENTSEV, Z. XU, C. PAN, M. ABDOU. Numerical and experimental studies of MHD flow in a rectangular duct with a non-conducting flow insert. Magnetohydrodynamics, vol. 46 (2010), No. 1, pp. 99-111.
5. Z. XU, C. PAN, X. ZHANG, L. ZHAO, J. ZHANG, G. YANG. Primary experimental results of MHD flow in the duct with flow channel insert. Nuclear Fusion and Plasma Physics, vol. 29 (2009), pp. 6-9 (in Chinese).
6. R. MOREAU. *Magnetohydrodynamics*, pp. 158, Kluwer Academic Publishers, Dordrecht, Netherlands (1990).